

3D Numerical Models for Along-axis Variations in Diking at Mid-Ocean Ridges

Thesis proposal

Xiaochuan Tian

Center for Earthquake Research and Information
The University of Memphis

xtian@memphis.edu

February 5, 2015

Abstract

Bathymetry of ocean floors reveals a great variety of morphologies at Mid-ocean Ridges (MORs). Previous studies showed that the morphologies at slow spreading MORs are mainly controlled by the ratio between rates of magma supply and plate extension. 2D models for the across-ridge cross-sections have been successful in explaining many of the observed morphological features such as abyssal hills and oceanic core complexes. However, the magma supply varies along the ridge and the interaction between the tectonic plates and magmatism at MORs are inevitably 3D processes. We propose to investigate the consequences of the along-axis variability in diking in terms of faulting pattern and the associated structures. This work will include implementation of an algorithm of parameterizing repeated diking in a 3D parallel geodynamic modeling code.

Contents

1	Introduction	1
2	Proposed Work	5
2.1	Method of Approach	5
2.2	Model Setup	6
2.3	Parameters to Control	7
3	Work Plan	8

1 Introduction

Around 70% of the Earth's crust is oceanic crust and the mid-ocean ridges (MORs), the longest mountain chains on the Earth, are where new crust are forming with a multitude of seismic and volcanic activities. To study how new crust is created and how MORs evolve is significant for Earth Sciences. Geodynamic modeling along with a variety of geological, geophysical observation and lab experiment constraints have been used to study how the MORs work as a system under geological time scale.

High-resolution multi-beam bathymetry has revealed various characteristics of topography along and across MOR axis. Three specific questions stimulate people's interests most. First, what causes the distinct difference in axial topography between slow and fast spreading ridges. Second, for slow spreading ridges, why does topography along ridge varies and how to explain many features observed. Third, why do oceanic core complexes (OCCs) form and what is the mechanism.

According to [Fowler, 2004], variations in mid-ocean ridge morphologies are mainly controlled by four factors: magma supply, tectonic strain, hydrothermal circulation and spreading rate. Among them, the spreading rate is the most important. Slow-to-intermediate spreading centers (half spreading rate less than 4cm/year) produce median valleys that are typically 10~20km wide and 1~2km deep (e.g., Mid-Atlantic Ridges, Figure 1(a)). Fast-spreading centers (half spreading rate greater than 5cm/year) have axial highs that are 10~20 km wide, 0.3~0.5 km high (e.g., East Pacific Rise, Figure 1(b)).

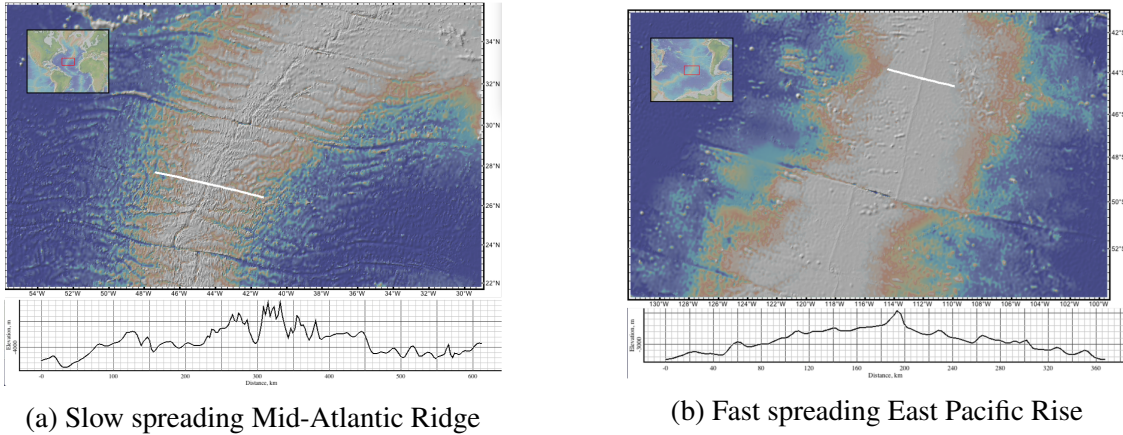


Figure 1: Profiles of bathymetry across MORs.

Slow spreading ridges exhibit along-axis variations as well in terms of the width and depth of median valleys and the off-axis morphology. Figure 2 shows that the topographic profile nearer to the center of the ridge segment (A-A') is rather symmetric and has higher frequency. The maximum relief is about 1km. In contrast, the near-tip profile (B-B') is asymmetric and has much lower frequency and a greater relief (~ 3 km). The bathymetry and crustal thickness along the ridge valley also varies. From [Chen and Lin, 1999], the maximum along-axis variation in crustal thickness ΔH_c is linearly increasing with segment length L , and the relationship is $\Delta H_c(L) = 0.0206L$ (Figure 3).

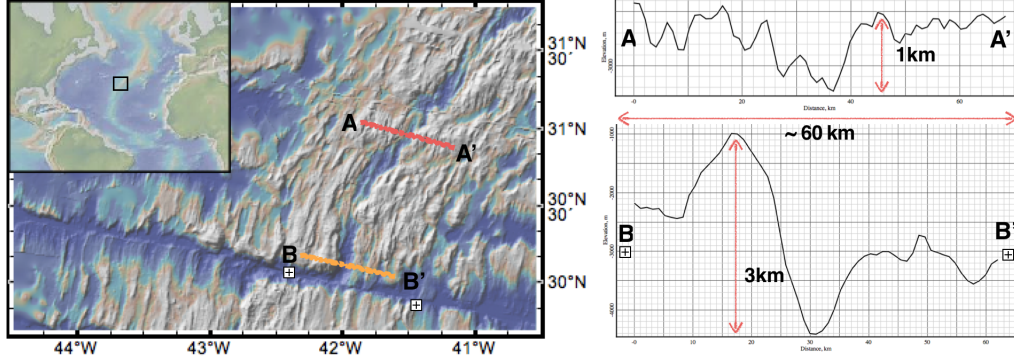


Figure 2: Two bathymetry cross-sections of Mid-Atlantic Ridge (MAR) with 10 times vertical exaggeration. A-A' is closer to the ridge segment center while B-B' is at the tip of the segment near the Atlantis Transform fault.

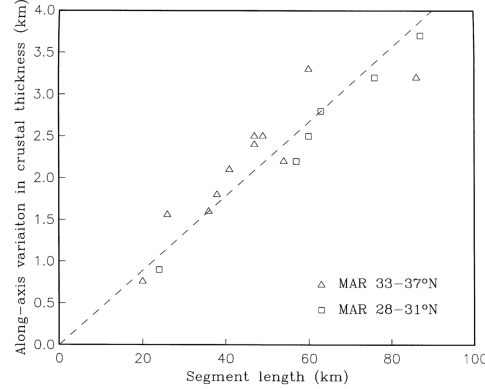


Figure 3: Relationship between the maximum crustal thickness variations along a ridge segment and the segment length. The dashed line is the best-fit linear regression of the combined data. [Chen and Lin, 1999]

Magma supply at MORs is mostly a passive process when no hot plume presents [Fowler, 2004]. Hot mantle rises up to fill the vacated room being created by plate separation and decompression will lead to partial melting of the hot mantle. The melt upwells due to both pressure difference and buoyancy from lateral density difference. When the melt solidifies near the surface, it forms new crust. This diking process can also release extensional stresses result from far-field driving forces.

The passive nature of magma supply results in the major difference between fast and slow spreading ridges in the amount of magma supply. At the fast spreading ridges, magma supply is always sufficient for accommodating plate separation by filling the space by dikes. However, the amount of magma supplied in the form of dikes is not as much at slow spreading ridges and the oceanic lithosphere experiences internal deformations (i.e. tectonics process like normal faulting) when the accumulated extensional stress exceeds the strength of the crust.

Buck et al. [2005] attributed the contrasting faulting patterns and ocean floor morphology of fast- and slow-spreading ridges to the difference in the amount of plate extension accommodated by diking. They defined the ratio between the rates of diking and plate separation as $M = V_{dx}/2V_x$, where V_{dx} is the extensional velocity of a widening dike and V_x is the half spreading rate of the

MOR. According to this definition, $M = 1$ represents the case where diking is frequent enough to release all the tensional stresses from plate separation. $M = 0$ corresponds to the case of no magma supply, in which diking does not account for any of the plate motion and therefore plates kinematics requires plates to go through internal deformations. As shown in Figure 4, an axial high forms at a fast spreading ridge ($M=1$) due to buoyancy from lateral density difference across ridge axis but a median valley forms at a slow-spreading ridge ($M=0.5$) due to near-axis normal faulting, which is in turn caused by the stretching of oceanic lithosphere.

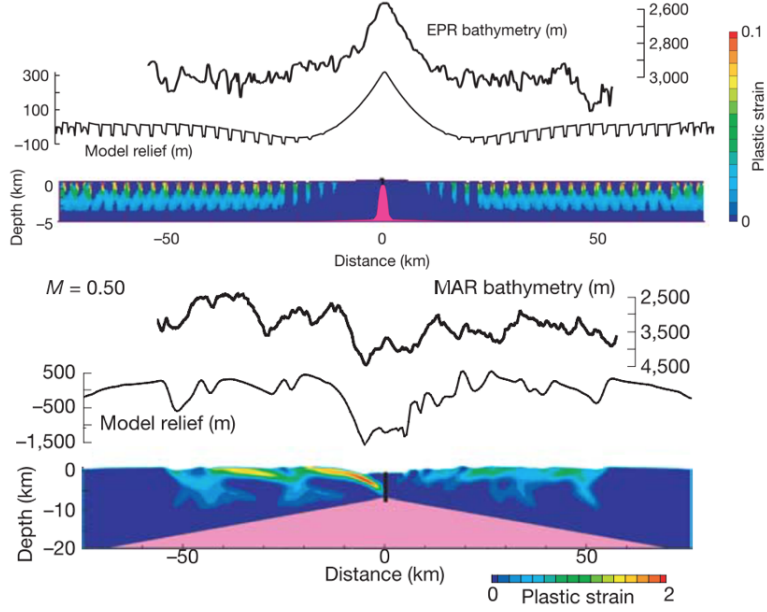


Figure 4: Upper one: modeling result for fast spreading agrees well with the observation of East Pacific Rise. Lower one: modeling result for slow spreading ridges agrees well with the bathymetry of Mid Atlantic Ridge. [Buck et al., 2005]

Tucholke et al. [2008] expanded investigation on the role of M in the mid-ocean ridge mechanics. They focused on faulting behaviors of slow spreading ridges and find that the OCCs are most likely to form when M varies from 0.3 to 0.5. As shown in Figure 5, when $M=0.7$, repeated diking pushes faults forming at the spreading center away from axis. Since the thickness of the brittle layer increases away from the ridge axis, frictional and bending energy for maintaining the fault also increases. When it exceeds the energy for breaking a new near-axis fault, the old fault will be replaced by the new one. When $M=0.3\sim0.5$, the normal faults remains active for a long time to become detachment faults, exhume the lower crust and mantle materials to the seafloor. When M is less than 0.3, most of the tension is accommodated by intra-plate deformations rather than by diking and as a result, faulting pattern is more complicated and unsteady.

The M -factor formulation used in these previous 2D models successfully explained major features found in across-ridge profiles of seafloor bathymetry. However, 2D models have limitations in studying the along ridge-axis interactions, especially when important variables are not constant along the ridge axis. Magma supply at fast spreading ridges seems always sufficient for accommodating plate motions with little variation along the ridge axis. The relatively uniform topography along fast spreading ridges is considered to be consistent with the uniformly abundance of magma

supply. However, along slow spreading ridges, bathymetry, gravity anomaly, reflection and refraction seismology show good correlation with variation in crustal thickness [Ryan et al., 2009, Chen and Lin, 1999, Lin et al., 1990, Tolstoy et al., 1993]. Because oceanic crust is mainly formed by upwelled magma at the ridge, variation in the thickness of the crust implies variation in magma supply. At slow spreading ridges, hydrothermal cooling, thermal structures and even local spreading rate [Baines et al., 2008] also varies both along and across the ridge axis and they appear interrelated. Thus, for slow-to-intermediate spreading ridges, the interactions between tectonics and magmatism at MORs are inevitably 3D processes and 3D numerical models are desirable for better understanding factors controlling both across- and along-ridge variations.

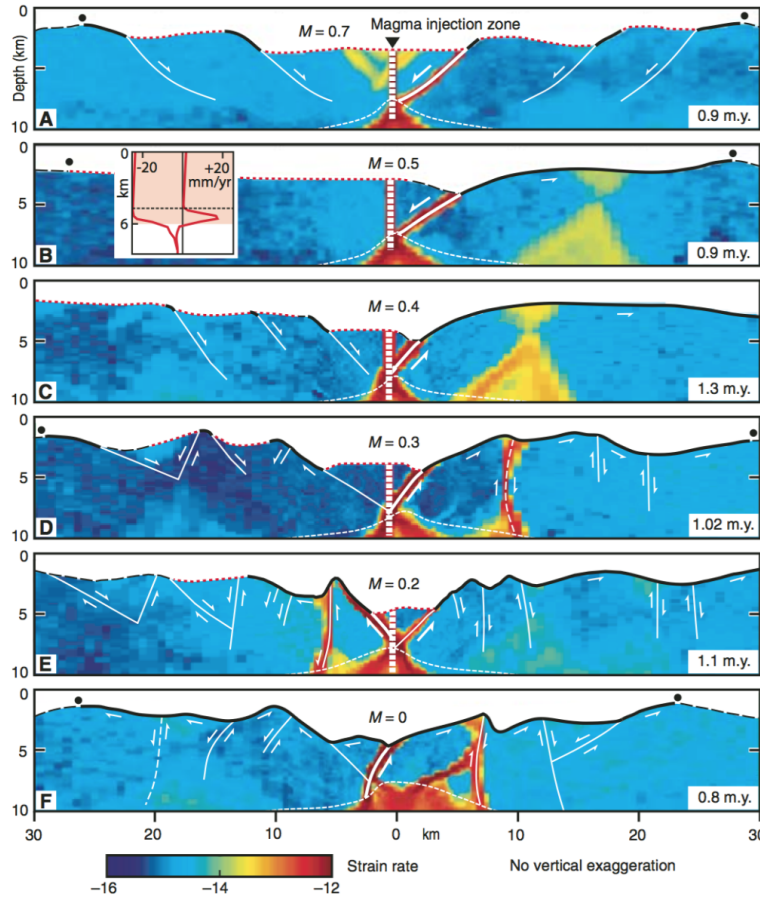


Figure 5: A~F: Faulting behavior for different values of M . Geologic interpretation is superimposed on modeled distribution of strain rate. Dots show breakaways of initial faults. Dashed seafloor is original model seafloor, red dotted seafloor is formed dominantly by magmatic accretion, and solid bold is fault surface. Note that detachment faults in B and C are not interrupted by secondary faults. [Tucholke et al., 2008]

2 Proposed Work

The purpose of this thesis is to study how the along-ridge variation in M will make a contribution to the observed various topography assuming that M is the first order control over the topography evolution of MORs governing the interaction between magmatism and tectonic deformations. We will extend the M-factor formulation originally developed for 2D models to 3D by implementing it into a 3D numerical modeling code SNAC [Choi et al., 2008]. We will focus on studying the last two questions mentioned in the introduction: 1) why does topography along ridge varies and how to explain many features observed; 2) why do OCCs form and what is the mechanism.

By systematically exploring the behaviors of the 3D models and comparing them with observations, we will be able to better understand how the mid-ocean ridge magmatism and tectonic deformations interact.

2.1 Method of Approach

The numerical modeling code, SNAC, is an explicit Lagrangian finite element code. It solves the force balance equation for elasto-visco-plastic materials. Figure 6 shows major parts of the SNAC's algorithm.

For each time step dt , strain and strain rates are updated based on the boundary conditions shown in Figure 7. A constitutive model returns updated stresses corresponding to these deformation measures. Internal forces are then calculated from the update stresses, which is plugged into the momentum balance equation together with the body force term. Then, the net force divided by internal mass yields acceleration at a node point, which is time-integrated to velocity and displacement.

A 3D domain is discretized into hexahedral elements, each of which is in turn divided into two sets of tetrahedra. This symmetric discretization prevents faulting from favoring a specific direction or “mesh grains”.

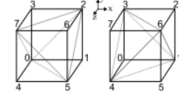
Rheology for the oceanic lithosphere is assumed to be elasto-visco-plastic. When viscosity is high at low temperature, the rheology essentially becomes the Mohr-Coulomb plasticity with strain softening and thus can create shear bands that behave like faults. Strain softening is realized by cohesion decreasing with increasing amount of permanent (i.e., plastic) strain. We assume this relationship is linear for simplicity such that it is sufficient for a full description of strain weakening to define initial and final values of cohesion and a critical plastic strain at which cohesion becomes the final value. We define the rate of strain weakening as the cohesion difference divided by the critical plastic strain and use it as one of the model parameters. When temperature is high and viscosity is low, the rheology becomes the Maxwell viscoelasticity and can model creeping flow. By assuming an appropriate initial temperature distribution, we can effectively set up a structure of a brittle lithosphere and a ductile asthenosphere. Rheological parameters are taken from previous studies that used a similar rheology [Buck 2005; Tuckholke et al., 2008] or from lab experiments [e.g., Kirby and Kronenberg, 1987].

For 3D diking processss, the expanding strain $\Delta\varepsilon_{xx}$ results from diking at the ridge will lead to extra-stresses in all three directions $\Delta\sigma_{xx}$, $\Delta\sigma_{yy}$ and $\Delta\sigma_{zz}$ based on the constitutive equations $\sigma_{ij} = \delta_{ij}\lambda\varepsilon_{ij} + 2\mu\varepsilon_{ij}$.

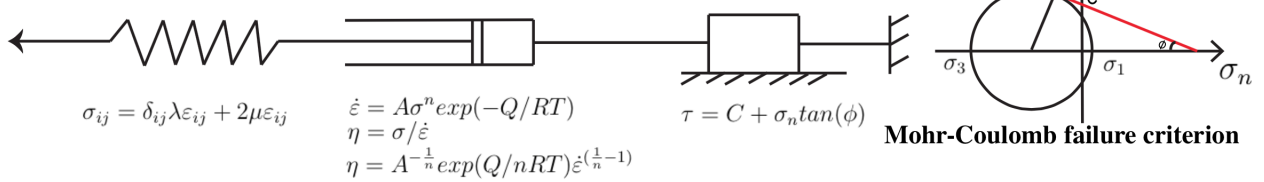
SNAC: a 3D, MPI parallelized, updated Lagrangian explicit finite difference code for modeling long-term tectonic evolution of the Earth's elasto-visco-plastic crust and mantle. (Choi et al., 2008)

Momentum Balance Equation: $\frac{\partial \sigma_{ij}}{\partial x_j} + \rho g_i = \rho \frac{Dv_i}{Dt}$

Spatial Decritization: A 3D domain is discretized into hexahedral elements, each of which is filled with two sets of 5 tetrahedra.



Elasto-Visco-Plastic (EVP) Rheology:



Diking M Formulation: $M = Vdx / 2Vx$ (Vdx is the diking velocity in x direction, 2Vx is the full spreading velocity)

Stresses introduced by a dike accretion strain(dike widening) $\Delta\epsilon_{xx}$ in each time step dt:

$$\Delta\sigma_{xx} = (\lambda + 2\mu)\Delta\epsilon_{xx} \quad \Delta\sigma_{yy} = \lambda\Delta\epsilon_{xx} \quad \Delta\sigma_{zz} = \lambda\Delta\epsilon_{xx}$$

Figure 6: Essential components of the numerical method to be used for the proposed research

2.2 Model Setup

I propose the model setup shown in Figure 7. Temperature linearly increases from 0 °C at the top surface to 240 °C at the depth of 6 km, reflecting enhanced cooling due to hydrothermal circulation. Below 6 km, the temperature profile follows the semi-infinite half-space cooling model of moving plates [e.g., Turcotte and Schubert, 2002]. Two sides perpendicular to the z coordinate axis are free-slip. The top surface has a vertical traction from water column, of which height is locally determined as 4000-h(x,z) m, where h(x,z) is the topography at a location, (x,z). The bottom surface is supported by the Winkler foundation. Temperature is fixed at 0°C on the top surface and at 1300°C on the bottom surface. We will adopt the power-law rheology of dry diabase[e.g., Kirby and Kronenberg, 1987, Buck et al., 2005].

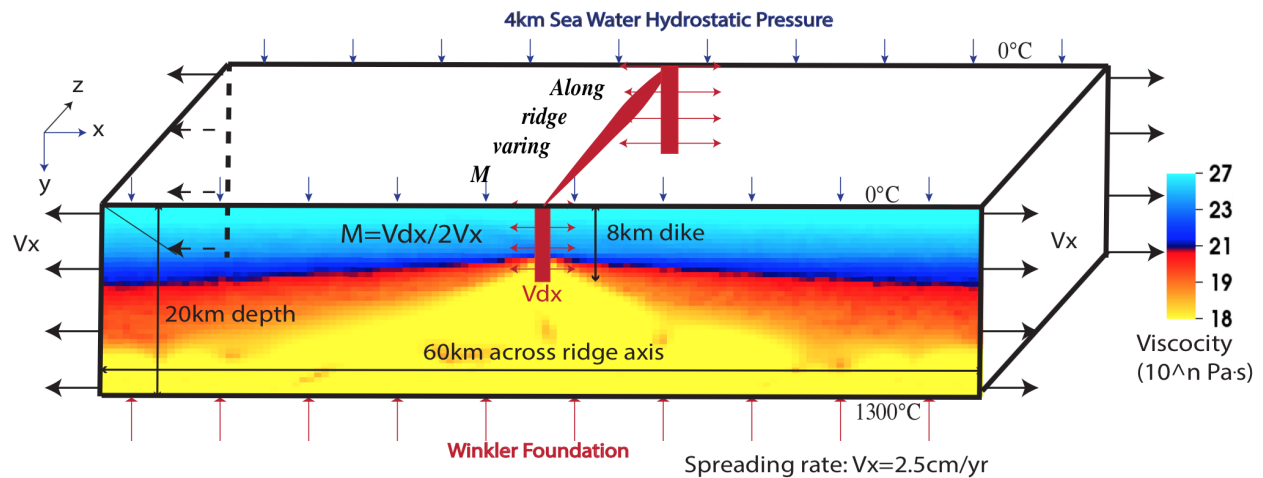


Figure 7: Preliminary model setup

2.3 Parameters to Control

Although how to estimate the M values from observations has not been well established, we do have constraints from a large dataset of bathymetry, gravity and seismic surveys as well as geological drilling. Generally, at slow spreading ridges, magma supplies mostly at the center of the ridge segment and decreases towards the end of the segment [Tolstoy et al., 1993, Chen and Lin, 1999]. There is also evidence for shorter wavelength of 10 to 20 km discrete focus of magma accretion along the ridge axis [Lin et al., 1990].

Based on these constraints, we can start considering only a few end-member scenarios of variations in M along the ridge axis. The variation in M is parametrized in terms of the functional forms (e.g. discrete increment, linear, sinusoidal and square root), its wavelength (e.g. 10km, 20km and 40km) and the ranges of M (e.g. 0.2 to 0.8, 0.5 to 0.7 and 0.5 to 0.8).

Preliminary pseudo-2D results show that the model behavior in faulting pattern is sensitive to the rate of strain weakening. Two cases of strain weakening will be tested in my thesis. In one case (denoted as Type 1), cohesion linearly decreases from 44 MPa to 4 MPa for plastic strain accumulating from 0 to 0.1. The other case (Type 2) assumes cohesion linearly decreasing from 44 MPa to 4 MPa for plastic strain accumulating from 0 to 0.33.

3 Work Plan

Table 1 shows what have been done so far and what still need to be finished for the completion of the research.

Timeline	Work	Progress
Dec., 2013~Jan., 2014	Understand the basics of MORs tectonics and magmatism system	completed
Jan., 2014~March, 2014	run 2D models in FLAC to understand the framework	completed
March, 2014~May, 2014	Learn C programing and continuum mechanics and understand the 3D code	completed
May, 2014~July, 2014	Benchmark pseudo 3D code with previous modeling results	completed
July, 2014~Sept., 2014	Implement varying M into 3D code SNAC	completed
Sept., 2014~Nov., 2014	Run preliminary 3D models and explain the model behaviors	completed
Nov., 2014~Dec., 2014	Prepare AGU conference poster and presentation	completed
Jan., 2015~Feb., 2015	Run models with different scenarios of M and systematically examine how M affects the topography	ongoing
Feb. 2015~March, 2015	Thesis writting	ongoing
April. 2015	Thesis defense	

Table 1: An overview of what have been done and plan for what need to be done

References

- G. Baines, M. J. Cheadle, B. E. John, and J. J. Schwartz. The rate of oceanic detachment faulting at atlantis bank, sw indian ridge. *Earth and Planetary Science Letters*, 273(1-2):105–114, Aug. 2008. ISSN 0012821X. doi: 10.1016/j.epsl.2008.06.013.
- R. Buck, L. Lavier, and A. Poliakov. Modes of faulting at mid-ocean ridges. *Nature*, 434(7034):719–23, 2005. ISSN 1476-4687. doi: 10.1038/nature03358.
- Y. J. Chen and J. Lin. Mechanisms for the formation of ridge-axis topography at slow-spreading ridges: A lithospheric-plate flexural model. *Geophysical Journal International*, 136:8–18, 1999. ISSN 0956540X. doi: 10.1046/j.1365-246X.1999.00716.x.
- E. Choi, L. Lavier, and M. Gurnis. Thermomechanics of mid-ocean ridge segmentation. *Physics of the Earth and Planetary Interiors*, 171(1-4):374–386, Dec. 2008. ISSN 00319201. doi: 10.1016/j.pepi.2008.08.010.
- C. M. R. Fowler. *The solid earth: an introduction to global geophysics*. Cambridge University Press, 2004.
- S. Kirby and A. K. Kronenberg. Rheology of the lithosphere: Selected topics. *Reviews of Geophysics*, 25(6):1219–1244, 1987.
- J. Lin, G. M. Purdy, H. Schouten, J.-C. Sempere, and C. Zervas. Evidence from gravity data for focused magmatic accretion along the Mid-Atlantic Ridge. *Nature*, 344:627–632, 1990. ISSN 0028-0836. doi: 10.1038/344627a0.
- W. B. F. Ryan, S. M. Carbotte, J. O. Coplan, S. O’Hara, A. Melkonian, R. Arko, R. A. Weissel, V. Ferrini, A. Goodwillie, F. Nitsche, J. Bonczkowski, and R. Zemsky. Global multi-resolution topography synthesis. *Geochemistry, Geophysics, Geosystems*, 10, 2009. ISSN 15252027. doi: 10.1029/2008GC002332.
- M. Tolstoy, A. J. Harding, and J. A. Orcutt. Crustal Thickness on the Mid-Atlantic Ridge: Bull’s-Eye Gravity Anomalies and Focused Accretion. *Science*, 262(October):726–729, 1993. ISSN 0036-8075. doi: 10.1126/science.262.5134.726.
- B. E. Tucholke, M. D. Behn, W. R. Buck, and J. Lin. Role of melt supply in oceanic detachment faulting and formation of megamullions. *Geology*, 36(6):455, 2008. ISSN 0091-7613. doi: 10.1130/G24639A.1.
- D. L. Turcotte and G. Schubert. *Geodynamics*. Cambridge, 2002.